frontiers in Medicine

ORIGINAL RESEARCH
published: 09 June 2021
doi: 10.3389/fmed.2021.679171

Urinary Extracellular Vesicles for Renal Tubular Transporters Expression in Patients With Gitelman Syndrome

*Chih-Chien Sung[1], Min-Hsiu Chen[1], Yi-Chang Lin[2], Yu-Chun Lin[3], Yi-Jia Lin[3], Sung-Sen Yang[1] and Shih-Hua Lin[1]**

[1] Division of Nephrology, Department of Medicine, National Defense Medical Center, Tri-Service General Hospital, Taipei, Taiwan, [2] Division of Cardiovascular Surgery, Department of Surgery, National Defense Medical Center, Tri-Service General Hospital, Taipei, Taiwan, [3] Deparment of Pathology, National Defense Medical Center, Tri-Service General Hospital, Taipei, Taiwan

Background: The utility of urinary extracellular vesicles (uEVs) to faithfully represent the changes of renal tubular protein expression remains unclear. We aimed to evaluate renal tubular sodium (Na^+) or potassium (K^+) associated transporters expression from uEVs and kidney tissues in patients with Gitelman syndrome (GS) caused by inactivating mutations in *SLC12A3*.

Methods: uEVs were isolated by ultracentrifugation from 10 genetically-confirmed GS patients. Membrane transporters including Na^+-hydrogen exchanger 3 (NHE3), $Na^+/K^+/2Cl^-$ cotransporter (NKCC2), NaCl cotransporter (NCC), phosphorylated NCC (p-NCC), epithelial Na^+ channel β (ENaCβ), pendrin, renal outer medullary K1 channel (ROMK), and large-conductance, voltage-activated and Ca^{2+}-sensitive K^+ channel (Maxi-K) were examined by immunoblotting of uEVs and immunofluorescence of biopsied kidney tissues. Healthy and disease (bulimic patients) controls were also enrolled.

Results: Characterization of uEVs was confirmed by nanoparticle tracking analysis, transmission electron microscopy, and immunoblotting. Compared with healthy controls, uEVs from GS patients showed NCC and p-NCC abundance were markedly attenuated but NHE3, ENaCβ, and pendrin abundance significantly increased. ROMK and Maxi-K abundance were also significantly accentuated. Immunofluorescence of the representative kidney tissues from GS patients also demonstrated the similar findings to uEVs. uEVs from bulimic patients showed an increased abundance of NCC and p-NCC as well as NHE3, NKCC2, ENaCβ, pendrin, ROMK and Maxi-K, akin to that in immunofluorescence of their kidney tissues.

Conclusion: uEVs could be a non-invasive tool to diagnose and evaluate renal tubular transporter adaptation in patients with GS and may be applied to other renal tubular diseases.

Keywords: Gitelman syndrome, renal tubular transporters, hypokalemia, renal tubular disease, urinary extracellular vesicles (exosomes)

OPEN ACCESS

Edited by:
Zaid A. Abassi, Technion Israel Institute of Technology, Israel

Reviewed by:
Gerardo Gamba, National Autonomous University of Mexico, Mexico
Gautam Bhave, Vanderbilt University, United States

***Correspondence:**
Shih-Hua Lin
l521116@ndmctsgh.edu.tw

Specialty section:
This article was submitted to Nephrology, a section of the journal Frontiers in Medicine

Received: *11 March 2021*
Accepted: *11 May 2021*
Published: *09 June 2021*

Citation:
Sung C-C, Chen M-H, Lin Y-C, Lin Y-C, Lin Y-J, Yang S-S and Lin S-H (2021) Urinary Extracellular Vesicles for Renal Tubular Transporters Expression in Patients With Gitelman Syndrome. Front. Med. 8:679171. doi: 10.3389/fmed.2021.679171

INTRODUCTION

Gitelman syndrome (GS) is one of the most common inherited tubulopathy with a prevalence ranging from 0.25 to 4/10,000 per population. It is caused by biallelic inactivating mutations in the *SLC12A3* gene encoding thiazide-sensitive sodium-chloride cotransporter (NCC) expressed in the apical membrane of distal convoluted tubules (DCT) (1, 2). To date, more than 450 different mutations scattered throughout *SLC12A3* have been identified in GS (1, 3, 4). Clinical characteristics include renal sodium (Na^+) wasting with secondary hyperreninemia and hyperaldosteronism, renal potassium (K^+) wasting with chronic hypokalemia and metabolic alkalosis, and renal magnesium wasting with hypomagnesemia, but hypocalciuria (5). The defective NCC function caused by different classes of *SLC12A3* mutations leads to the reduced sodium chloride (NaCl) reabsorption in DCT with increased luminal NaCl delivery to downstream collecting ducts (CD) responsible for NaCl reabsorption via epithelial Na^+ channel (ENaC) and K^+ secretion via renal outer medullary K1 channel (ROMK) and large-conductance, voltage-activated and Ca^{2+}-sensitive K^+ channel (Maxi-K). Although the expression of ENaCβ, ROMK and Maxi-K in mouse GS model has been reported to be significantly increased in both immunoblotting and immunofluorescence of mouse kidney (6), the adaptive response of upstream and downstream Na^+ and K^+ associated transporters in response to renal Na^+ and K^+ wasting in GS patients remains unknown.

Urinary extracellular vesicles (uEVs) containing membrane and cytosolic proteins, mRNAs, miRNA and signaling molecules from each renal epithelial cell type may reflect the physiological state of their cells of origin (7, 8). The isolation of uEVs had the potential to shed much insight on the health status of the kidney and expression of urinary proteins (9–11). Knepper et al. has identified more than one thousand proteins including solute and water transporters, vacuolar H^+-ATPase subunits, and disease related proteins (12). It has been also reported that the isolated uEVs had an increased NCC abundance in patients with primary aldosteronism (13, 14) and Cushing syndrome (15) as well as a rapid increase in abundance of NCC and p-NCC in healthy subjects following the mineralocorticoid administration (16). In the inherited renal tubular disorders, uEVs have been used as a non-invasive tool to detect the defect of mutated renal tubular transporter such as NCC and $Na^+/K^+/2Cl^-$ cotransporter (NKCC2) expression in patients with GS and Bartter syndrome, respectively (17, 18). Nevertheless, uEVs for other renal Na^+ and K^+ associated transporters expression has not been also investigated in GS.

The aim of this study was to evaluate the changed expression of NCC, phosphorylated NCC (p-NCC), upstream DCT such as Na^+-hydrogen exchanger 3 (NHE3), NKCC2, downstream DCT such as ENaCβ, pendrin, as well as K^+-secreting channels such as ROMK and Maxi-K from uEVs and representative kidney tissues in patients with GS. Results to be reported indicated that a marked attenuation of NCC and p-NCC expression from uEVs could be used as a non-invasive diagnostic biomarker for GS. Both upstream NHE3 and downstream ENaCβ and pendrin from uEVs were increased in response to salt-losing and an enhanced ROMK and Maxi-K expression were associated with renal K^+ wasting in GS patients. These findings from uEVs were similar to those obtained from renal biopsied tissues in GS patients.

MATERIALS AND METHODS

Study Design

The study protocol was approved by the Ethics Committee on Human Studies at Tri-Service General Hospital (TSGHIRB No.2-103-05-160 and TSGHIRB No.2-105-05-062). We prospectively collected 10 genetically confirmed GS patients. Their mutations included homozygous intronic mutation ($n = 2$), compound heterozygous mutati on ($n = 8$) in the *SLC12A3* gene encoding NCC (**Table 1**). Five healthy controls and three bulimic patients as hypokalemic disease controls were also enrolled. The diagnosis of bulimia was based on the American Psychiatric Association's Diagnostic and Statistical Manual, Fifth Edition (19). Clinical characteristics and laboratory examination were collected and determined. Renal biopsied tissues were collected from three different GS patients with definite *SLC12A3* mutations (compound heterozygous mutation of intronic c1670-191/p.I888_H916del, p.T60M/p.R959fs, and p.T60M/splicing c.965-1G>A+c965-977gcggacattttgt>accgaaaattttt) and one bulimic patient. All of them had long-standing, severe hypokalemia refractory to aggressive K^+ supplementation and significant proteinuria. Control kidney tissue was obtained from normal part of kidney in one patient with renal cell carcinoma undergoing total nephrectomy.

uEVs Studies

Urine Collection and uEVs Isolation

Secondary morning spot urine with forty milliliters with protease inhibitors were collected for uEVs isolation by ultracentrifugation-based protocol. The urine sample was centrifuged at 17,000 × g for 10 min at 37°C. Supernatant was then ultracentrifuged at 200,000 × g for 2 h at 4°C. The pellet was resuspended in PBS or laemmli buffer with dithiothreitol.

Nanoparticle Tracking Analysis

Nanoparticles from isolated uEVs were analyzed using the NanoSight NS300 instrument (NanoSight Ltd, Amesbury, UK). Following published method (20), all experiments were carried out at a 1:1,000 dilution, yielding particle concentrations in the region of 1×10^8 particles ml^{-1} in accordance with the manufacturer's recommendations.

Transmission Electron Microscopy

uEVs pellet was carefully fixed the with enough volume of 2.5% glutaraldehyde (G5882, Sigma-Aldrich) in 0.1 M sodium cacodylate, pH 7.4 and 4% paraformaldehyde mix buffer (1:1) for 1 h at 4°C and then washed with PBS. Pre-fix the sample with 1 ml of 1% Osmium tetroxide (in ddH_2O) for 50 min at 4°C in dark. Post-fix the sample with 5% uranyl acetate (UA) blocking overnight at 4°C. Incubate for 10 min with a graded EtOH series (50, 70, 90, 95, 100%) and followed by EPON (Resin 20 ml, DDSA 7 ml, NMA 14 ml, DMP-30 0.8 ml). The uEVs samples

TABLE 1 | Characteristics of *SLC12A3* mutation among 10 patients with Gitelman syndrome.

Patients	Genotypes	Nucleotide change (NM_000339.3)	AA change (NP_000330.3)	Topological localization
1	Compound heterozygous	c.1924C>T + c.2548+253	p.R642C + Intronic	Transmembrane + C-terminal
2	Homozygous	c.1670-191C>T + c.1670-C>T	Intronic + Intronic	Transmembrane + Transmembrane
3	Compound heterozygous	c.2875_76delAG + c.2548+253	p.R959fs + Intronic	C-terminal + C-terminal
4	Compound heterozygous	c.2129C>A + c.2875-76delAG	p.S710X + p.R959fs	C-terminal + C-terminal
5	Compound heterozygous	c.488C>T+c.2660+1G>A	p.T163M + splicing	Transmembrane + C-terminal
6	Compound heterozygous	c.1000C>T+c.1326C>G	p.R334W + p.N442K	Transmembrane + Transmembrane
7	Homozygous	c.1670-191C>T + c.1670-C>T	Intronic+ Intronic	Transmembrane + Transmembrane
8	Compound heterozygous	c.2129C>A + c.2875_76delAG	p.S710X + p.R959fs	C-terminal + C-terminal
9	Compound heterozygous	c.911C>T/c.2875_76delAG	p.T304M + p.R959fs	Transmembrane + C-terminal
10	Compound heterozygous	c.2532G>A+c.805-06insTTGGCGTGGTCTCGG	p.W844X + p.T269delinsIGVVSA	C-terminal + Transmembrane

were analyzed with a Hitachi TEM HT7700 electron microscope operated at 60 kV.

Immunoblotting

For immunoblotting, the loading volume of each uEVs sample was adjusted so that the loaded amount of creatinine was constant (21, 22). SDS/PAGE was carried out on an 8% polyacrylamide gel, and proteins were transferred to Immobilon®-P membranes (Millipore, Amsterdam, The Netherlands). The primary antibodies were as follows: NSE (ab254088, Abcam, Cambridge, UK), TSG101 (ab125011, Abcam, Cambridge, UK), CD9 (GTX55564, Genetex, HsinChu City), AQP2 (sc-515770, Santa Cruz Biotechnology, Santa Cruz, CA), NHE3 (NHE31-A, Alpha Diagnostic Intl Inc., San Antonio, TX) (6), NKCC2 (AB2281, Millipore, Temecula, CA), NCC (AB3553, Millipore, Temecula, CA) (23), ENaCβ (ASC-019, Alomone labs, Jerusalem, Israel) (23), p-NCC (17T, in-house antibody) (23), Maxi-K (APC-021, Alomone labs, Jerusalem, Israel) (6), ROMK (APC-001, Alomone labs, Jerusalem, Israel) (6), and pendrin (ARP41739_P050, Aviva system biology, San Diego, CA). The membranes were incubated with the secondary antibody. Immunoreactive proteins were detected by the enhanced chemiluminescence method (Pierce, Rockford, IL, USA). The immunopositive bands from immunoblotting were quantified using pixel density scanning and calculated using Image J and the relative band intensity was normalized to the healthy controls.

Immunofluorescence of Kidney Tissue

After paraffin removal and rehydration, the slides were heated in 1× citrate buffer (ThermoFisher) and exposed to 3% H_2O_2 (ThermoFisher) at room temperature and then the blocking solution. After washing with PBS plus 0.1% Tween 20 (J.T. Baker), the tissue was incubated with primary antibodies at 4°C overnight. The primary antibodies of AQP2, NHE3, NKCC2, NCC, p-NCC, ENaCβ, Maxi-K, ROMK, and pendrin were used. The tissues were exposed to species-specific secondary antibodies conjugated to Alexa Fluor fluorophores (ThermoFisher). Immunofluorescence images were obtained by Zeiss LSM880 confocal microscope.

Statistical Analyses

Serum and urine biochemistry data were expressed as mean ± standard deviation. Correlation between uEVs particles and urine creatinine were calculated by Pearson's correlation coefficient statistic in Excel. Data analyses were performed with the Prism (v5) software (GraphPad Software). Group comparisons of renal transporters from uEVs between GS patients and healthy controls were made using a two-tailed unpaired Student's *t*-test. Statistical significance was defined as p-values <0.05.

RESULTS

Clinical Characteristics in GS

As shown in **Table 2**, all GS patients (Male/Female = 9/1, age 33.4 ± 7.8 years old) were normotensive with renal Na^+ and Cl^- wasting and secondary hyperreninemia (plasma renin activity, PRA 28.9 ± 14.4 ng/mL/h) but normal to high plasma aldosterone concentration (PAC) (229.4 ± 69.6 pg/mL), chronic hypokalemia (K^+, 2.34 ± 0.45 mmol/L) with higher urinary K^+ excretion (transtubular potassium gradient, 13.46 ± 10.91), metabolic alkalosis ($HCO3^-$, 28.7 ± 3.9 mmol/L), hypomagnesemia (Mg^{2+} 0.63 ± 0.07 mmol/L), and hypocalciuria (Ca^{2+}/Creatinine 0.07 ± 0.06 mmol/mmol).

Characterization of uEVs

Characterization of the uEVs in healthy controls was validated by nanoparticle tracking analysis (NTA), transmission electron microscopy (TEM), and immunoblotting of uEVs makers. NTA identified size distribution of particles in the expected uEVs size range of 20–120 nm shown in **Figures 1A,B**. The mean particle size and concentration were 132.9 ± 65.8 nm and 6.6 × 10^{14}/ml,

TABLE 2 | Clinical characteristics and biochemistries in patients with Gitelman syndrome.

Patients		1	2	3	4	5	6	7	8	9	10	Mean ± SD
SBP/DBP (mmHg)		123/65	111/68	120/80	114/78	128/70	120/64	126/64	120/70	105/84	115/68	116.2 ± 7.5/69.7 ± 7.4
Serum	Reference											
BUN (mmol/L)	2.50–8.93	5.71	5.36	7.85	4.64	6.07	5.36	7.14	4.64	4.28	5.71	5.68 ± 1.12
Creatinine (μmol/L)	61.9–106.1	79.6	88.4	114.9	53 0	106.1	106.1	88.4	97.2	70.7	97.2	90.17.0 ± 18.54
Sodium (mmol/L)	136–145	135	135	138	132	140	142	138	137	134	134	137.1 ± 3.1
Potassium (mmol/L)	3.5–5.1	2.6	1.9	2.4	2.9	2.8	2.3	2.1	2.1	1.5	2.8	2.34 ± 0.45
Chloride (mmol/L)	98–107	97	100	98	94	97	99	97	98	96	96	97.2 ± 1.7
Total Calcium (mmol/L)	2.15–2.55	2.33	2.20	2.33	2.35	2.53	2.45	2.50	2.23	2.45	2.45	2.38 ± 0.11
Magnesium (mmol/L)	0.7–1.05	0.53	0.66	0.62	0.62	0.70	0.66	0.74	0.58	0.62	0.53	0.63 ± 0.67
Hematocrit (%)	38.0–47.0	45.7	49.0	46.3	39.9	53.9	54.0	48.3	46.8	44.4	45.6	47.4 ± 4.3
Albumin (g/L)	35–57	43	37	43	48	47	46	43	38	46	45	44 ± 4
PRA (ng/ml/hr)	1.31–3.95	17.15	10.29	47.13	6.32	50.00	31.97	38.35	29.04	30.35	29.14	28.9 ± 14.4
PAC (pg/ml)	70–350	252	206	140	147	134	266	304	320	288	237	229.4 ± 69.6
$HCO3^-$ (mmol/L)	24	31.6	27.2	30.7	28.0	33.0	26.8	28.0	22.6	24.1	35.1	28.7 ± 3.9
Urine												
Creatinine (mmol/L)		10.6	9.4	7.9	5.7	7.3	2.1	7.9	6.2	4.7	5.2	8.6 ± 3.8
Sodium (mmol/L)		172	53	58	66	64	46	96	32	42	199	82.8 ± 57.1
Potassium (mmol/L)		45	21	27	48	43	26	17	56	37	49	36.9 ± 13.3
Chloride (mmol/L)		143	86	93	67	44	59	51	35	77	207	86.2 ± 52.4
Calcium (mmol/L)		0.58	0.55	0.25	1.28	0.23	0.05	0.10	0.63	0.38	0.53	0.46 ± 0.35
Magnesium (mmol/L)		3.09	2.55	2.34	3.58	3.17	0.86	0.62	2.26	1.52	4.61	2.46 ± 1.23
TTKG		7.15	7.28	7.10	10.80	12.51	12.61	7.13	41.13	22.67	6.23	13.46 ± 10.91

SBP, systolic blood pressure; DBP, diastolic blood pressure; PRA, plasma renin activity; PAC, plasma aldosterone concentration; TTKG, transtubular potassium gradient.

respectively. uEVs number was correlated strongly with urine creatinine (r^2 for 0.81, $P < 0.0001$) shown in **Figure 1C**. TEM also confirmed the quality of uEVs isolated by ultracentrifugation (**Figure 1D**). To further validate the uEVs purification protocol, we evaluated four commonly used uEVs makers including AQP2, TSG101, NSE, and CD9 in immunoblotting shown in **Figure 1E**. Expression pattern of selected renal transporters including NHE3, NKCC2, NCC, p-NCC, ENaCβ, pendrin, ROMK, and Maxi-K in healthy controls were shown in **Figure 1F**.

uEVs for Renal Tubular Na^+ and K^+ Associated Transporter Expression in GS

Compared with healthy controls, GS patients with different biallelic mutations exhibited a markedly attenuated expression of NCC and p-NCC protein isolated from their uEVs, indicative of an impaired NCC expression and function in GS (**Figures 2A,B**). The expression of NHE3, ENaCβ, and pendrin significantly increased although NKCC2 was not significantly increased. For uEVs associated renal tubular K^+ associated transporter expression, GS patients had significantly increased ROMK and Maxi-K expression.

Renal Tubular Na^+ and K^+ Associated Transporter Expression From Kidney Tissues in GS

AQP2 used for a tubular maker of CD was clearly stained. Compared with control kidney tissue, the representative kidney tissues from GS patients showed obviously diminished expression in both NCC and p-NCC. The expression of NHE3, ENaCβ and pendrin was significantly increased (**Figure 3**). The expression of ROMK was increased and the Maxi-K unexpressed in control kidney tissue without hypokalemia was also significantly enhanced in three GS patients. Overall, these finding from immunofluorescence of kidney tissues supported the findings of the isolated uEVs to examine Na^+ and K^+ associated renal transporter adaptation in GS patients.

Tubular Transporter Expression From uEVs and Kidney Tissue in Bulimic Patients

Three bulimic patients (male/female = 2/1, age 23.3 ± 4.0 years old) with normotension (systolic blood pressure 102 ± 17 mmHg, diastolic blood pressure 63 ± 5 mmHg) exhibited chronic hypokalemia (K^+ 2.73 ± 0.55 mmol/L), metabolic alkalosis ($HCO3^-$, 46.6 ± 11.9 mmol/L), with secondary hyperreninemia (PRA 4.3 ± 1.3 ng/mL/h) but normal to high PAC (127.6 ± 26.7 pg/mL). They all exhibited higher urinary K^+ excretion, high Na^+ (120.3 ± 80.4 mmol/L) but low Cl^- (18.7 ± 6.4 mmol/L), alkaline urine (bicarbonaturia), indicative of recent vomiting. As shown in **Figure 4A**, uEVs from them showed an increased abundance of NCC and p-NCC as well as NHE3, NKCC2, ENaCβ, pendrin, ROMK and Maxi-K. Immunofluorescence of the kidney tissue from a representative bulimic patient also had the similar finding to those in uEVs (**Figure 4B**).

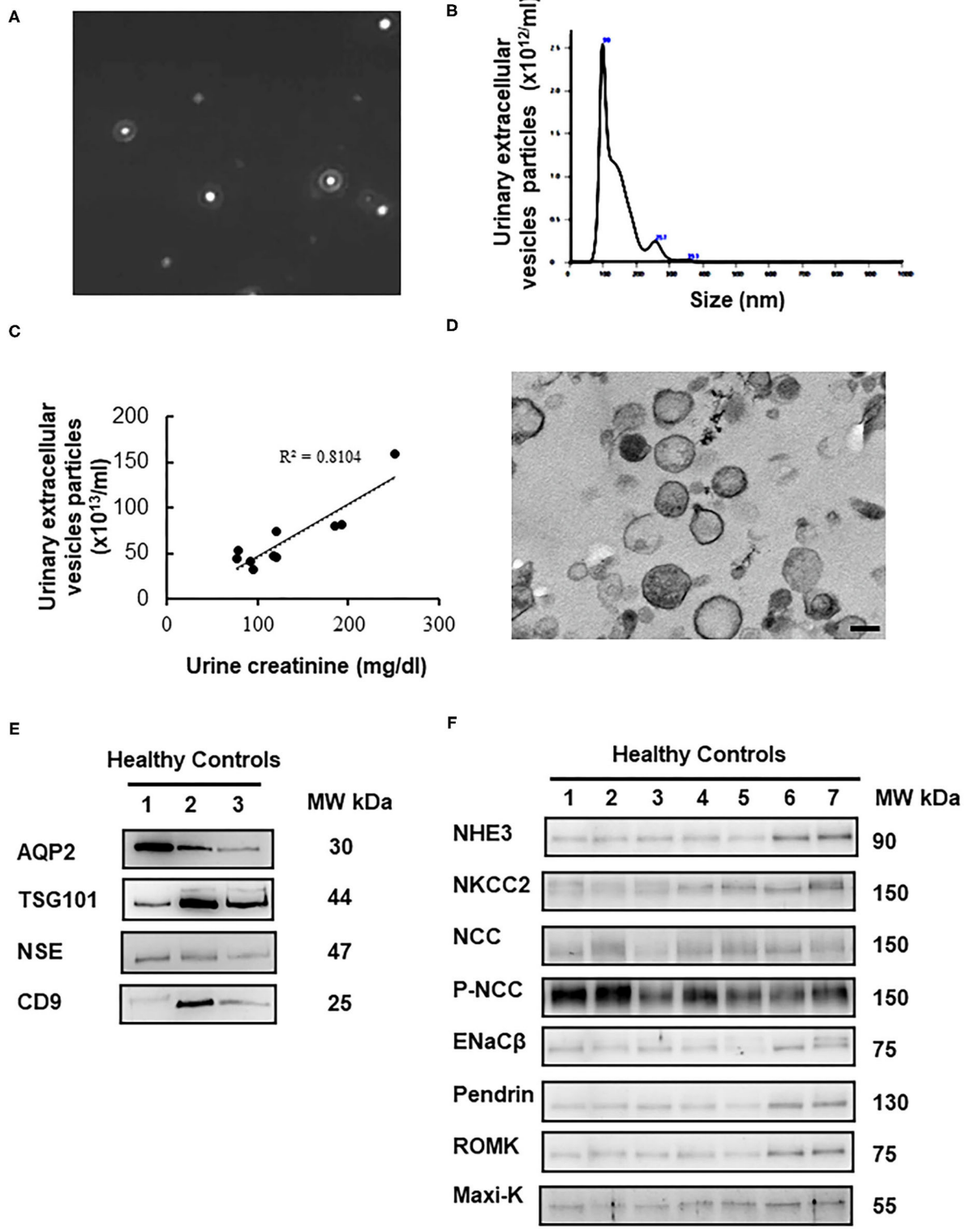

FIGURE 1 | Characterization of urinary extracellular vesicles (uEVs) from healthy controls. **(A)** Screen shot from 1:2,000 diluted urine sample reveals a range of particle sizes by nanoparticle tracking analysis (NTA). **(B)** Concentration and size distribution of uEVs (0–150 nm diameter) by NTA were shown. The concentration is expressed as number of particles per ml. **(C)** uEVs particles were correlated strongly with urine creatinine (r^2 for 0.81, $P < 0.0001$). **(D)** Transmission electron microscopy of uEVs was shown (scale bar 100 nm). **(E)** uEVs markers (AQP2, TSG101, NSE, and CD9) were assessed by immunoblotting. **(F)** Expression pattern of renal transporters including NHE3, NKCC2, NCC, p-NCC, ENaCβ, pendrin, ROMK, and Maxi-K from healthy controls was similar.

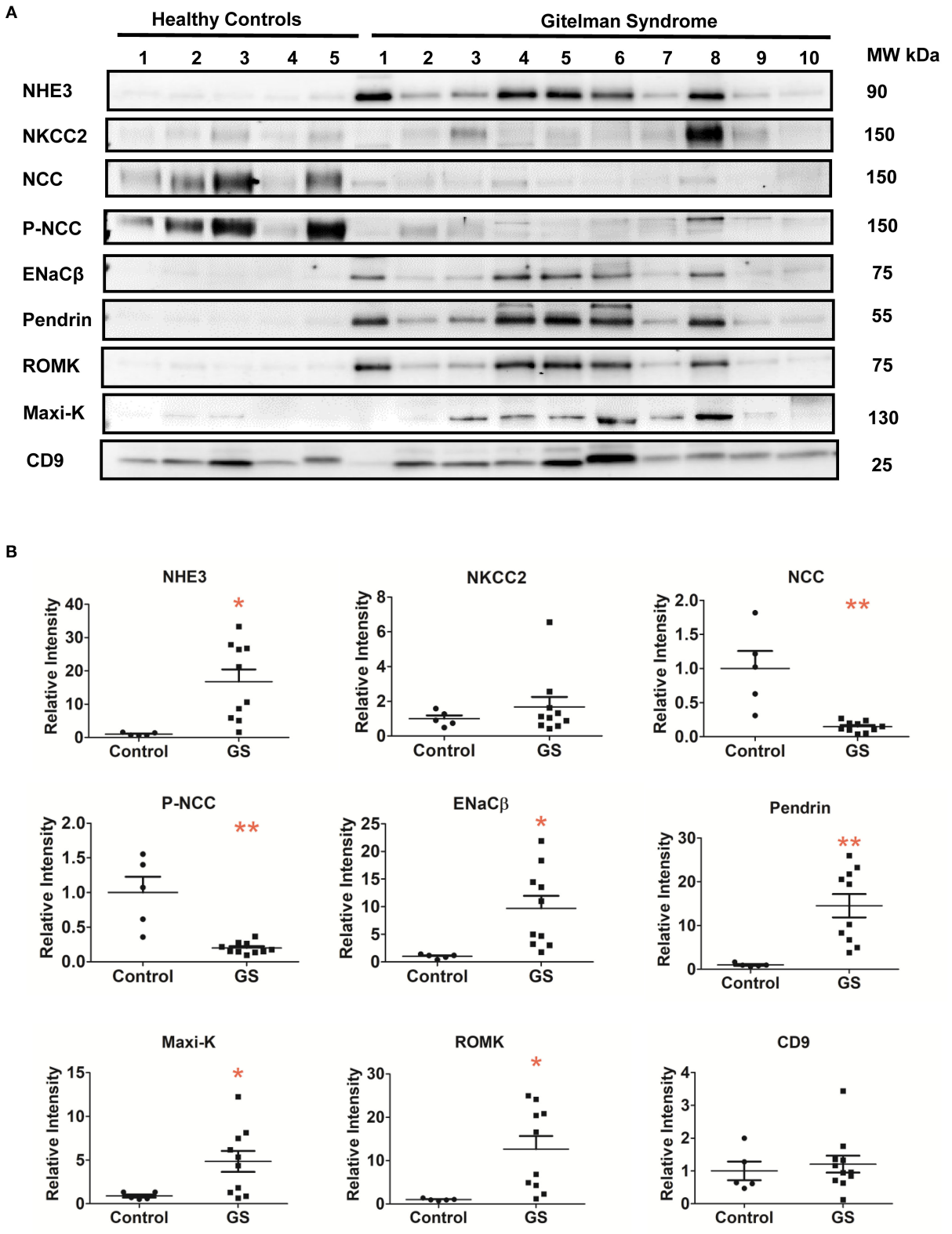

FIGURE 2 | Renal Na^+ and K^+ associated transporters expression from urinary extracellular vesicles in patients with GS ($n = 10$) compared with healthy controls. **(A)** Immunoblotting of renal transporters (NHE3, NKCC2, NCC, p-NCC, ENaCβ, pendrin, ROMK, Maxi-K, and CD9). **(B)** Quantification of immunoblotting of NHE3, NKCC2, NCC, p-NCC, ENaCβ, pendrin, ROMK, Maxi-K, and CD9. Error bars, standard deviation. $^*P < 0.05$, $^{**}P < 0.01$.

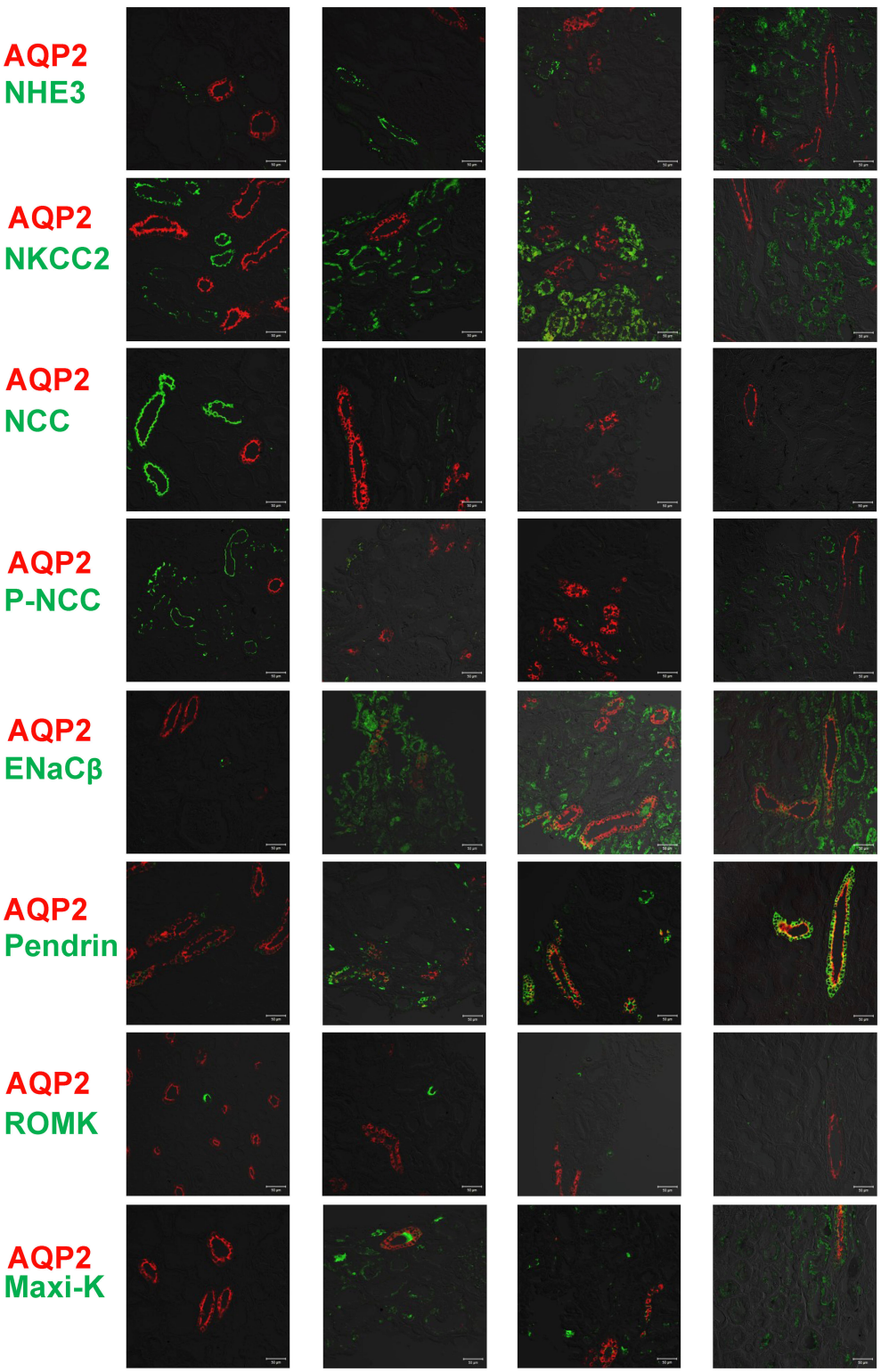

FIGURE 3 | Immunofluorescence of biopsied kidney tissues from another 3 representative GS patients (GS 1, GS 2, and GS 3) compared with the control kidney tissue. Renal transporters including NHE3, NKCC2, NCC, p-NCC, ENaCβ, pendrin, ROMK, Maxi-K were stained with green. AQP2 was stained with red for localization. Scale bar, 50 μm.

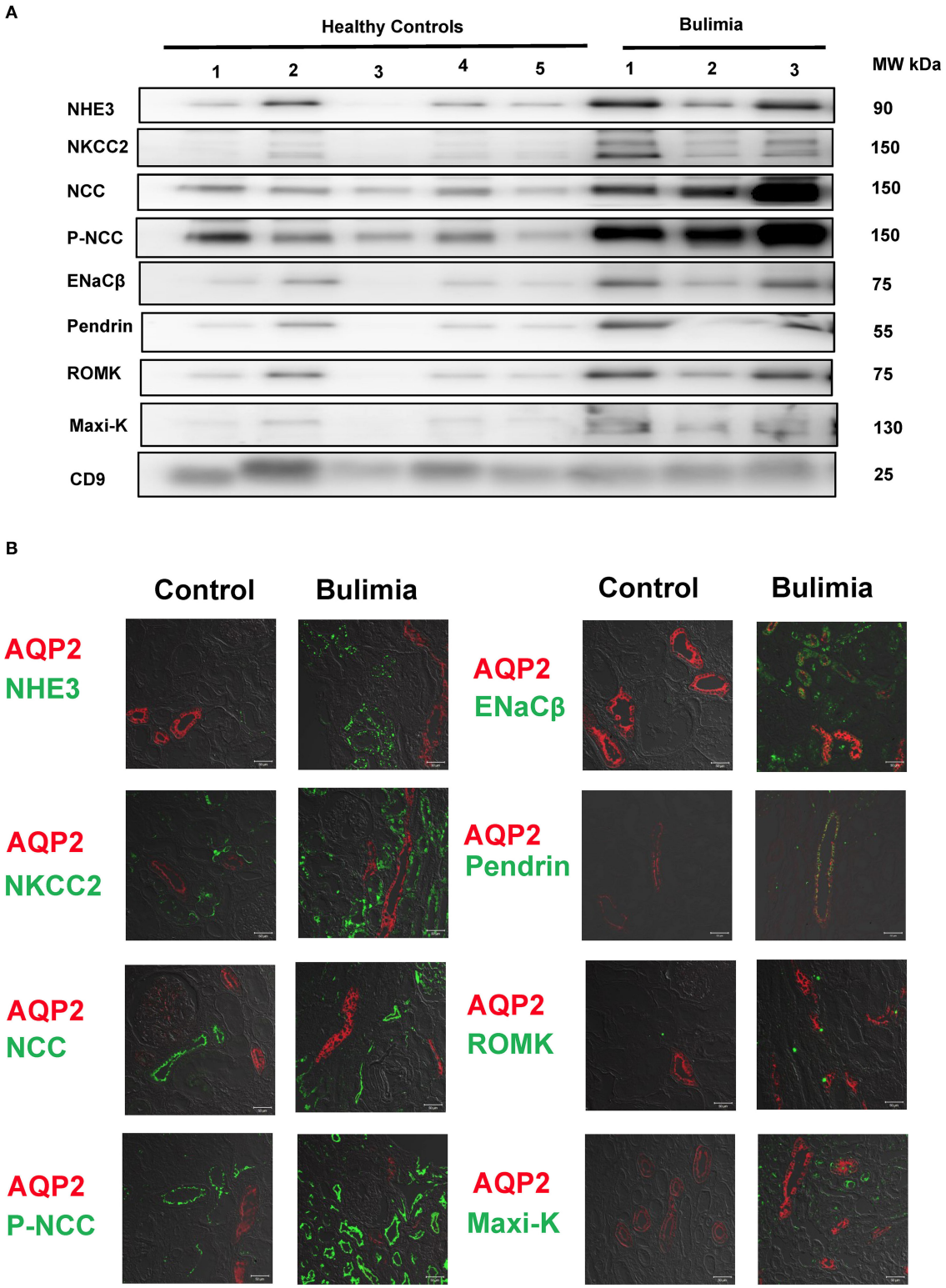

FIGURE 4 | Renal transporters expression from urinary extracellular vesicles (uEVs) and immunofluorescence of biopsied kidney tissues from bulimic patients. **(A)** Immunoblotting of renal transporters (NHE3, NKCC2, NCC, p-NCC, ENaCβ, pendrin, ROMK, Maxi-K, and CD9) from uEVs in bulimic patients ($n = 3$) compared with healthy control. **(B)** Immunofluorescence of NHE3, NKCC2, NCC, p-NCC (green, **right**) and ENaCβ, pendrin, ROMK, Maxi-K (green, **left**) from one representative bulimia patient compared with the control. AQP2 was stained with red for localization. Scale bar, 50 μm.

DISCUSSION

In this study, the isolated uEVs from GS patients with biallelic *SLC12A3* mutations showed the markedly attenuated expression of NCC and p-NCC whereas those from non-GS bulimic patients did a significantly enhanced abundance of NCC and p-NCC. In response to renal salt loss, the expression of upstream NHE3 and downstream ENaCβ, and pendrin were all accentuated. The abundance of ROMK and Maxi-K expression were also augmented for renal K^+ wasting in GS. Immunofluorescence of the representative kidney tissues from GS and bulimic patients also demonstrated similar findings to those from uEVs. This study might be the first to assess the abundance of renal tubular Na^+ and K^+ associated transporters from uEVs and kidney tissues in GS patients.

GS caused by inactivating *SLC12A3* mutations has an impaired NCC expression and/or activity as shown in both *vitro* and *vivo* studies. Although normal NCC expression with an impaired functional activity was shown in oocytes overexpressed T60M mutation at the critical NCC phosphorylation site, a markedly decreased total NCC and p-NCC protein abundance was evident in NccT58M/T58M GS knock-in mice and in the urine of human GS with homozygous T60M mutations (23). In addition, the reduced or abolished NCC abundance on the apical membrane of DCT from the human kidney tissues in GS patients with *SLC12A3* mutations were also demonstrated (24, 25). These findings supported the notion that the reduced expression of NCC was a biomarker for GS despite different mechanisms involved in the impaired NCC protein synthesis (24, 26), and sorting or trafficking defect of NCC (27). Accordingly, it is important to find a non-invasive method to faithfully represent NCC abundance in GS. Previous studies using uEVs to measure the mutated NCC by immunoblotting and enzyme-linked immunosorbent assays (ELISAs) in GS patients only showed the decreased NCC abundance (17, 18). In this study, the isolated uEVs from GS patients revealed that both NCC and p-NCC abundance were markedly diminished, also confirmed by the human kidney tissue of genetically-confirmed GS patients.

It is of great interest to understand and localize the tubular adaptation in the inherited renal tubular disorders. The traditional methods were the preparation of whole kidney sections for immunostaining and immunoblotting or biotinylating the rat or mice kidney tissues *in situ* under various chronic conditions in animal models. Tubular adaptation to renal Na^+ loss has been evaluated in the distal tubules in experimental models of GS but not human GS. Knepper et al. has used the LC-MS/MS to profile the proteome of human uEVs and suggested that uEVs analysis be a potential approach to discover adaptation in renal transporters (12). Using uEVs analysis in GS, we found that the abundance of upstream NHE3 in the proximal tubules (PT) necessary for bicarbonate reabsorption, salt and fluid homeostasis was significantly increased (28–30). Renal NHE3 abundance was markedly increased in K^+-depleted rats (31), indicating that NHE3 expression can be also regulated by the hypokalemia independent of volume depletion. Similarly, downstream ENaCβ in the principal cells of CD for tubular salt reabsorption was enhanced (32, 33). Of note, pendrin as a $Cl^-/HCO3^-$ exchanger expressed in the apical region of distal tubules and involved in the tubular Cl^- absorption and $HCO3^-$ secretion was augmented (34). Activation of pendrin-mediated Cl^- absorption has also been reported in NCC KO mice (35). Although pendrin expression has been examined in many rodent treatment models such as NCC KO mice, an aldosterone infusion or the administration of $NaHCO_3$ to regulate acid-base and salt regulation, our study suggested the increased pendrin expression from uEVs and biopsied kidney tissues be responsive to renal salt wasting and also chronic metabolic alkalosis in GS patients.

K^+ excretion in distal nephron is driven by either voltage-dependent ROMK and/or flow dependent Maxi-K (36). ROMK is an inwardly rectifying K^+ channel (37) traditionally responsible for the main renal K^+ secretory channel, dependent on Na^+ delivery and driven by electrogenic ENaC-mediated Na^+ reabsorption (38–40). Maxi-K is flow-stimulated K^+ secretion and activated by an increase in intracellular calcium and membrane depolarization (41, 42). Defective NaCl absorption in DCT leads to the increased flow rate to downstream connecting tubules (CNT) and CD to naturally stimulate both ROMK and Maxi-K. In animal model of GS (Ser707X knockin mice), an enhanced expression of both ROMK and Maxi-K has been clearly shown (6). Our uEVs for the expression of both ROMK and Maxi-K abundance were significantly increased in GS patients, akin to the findings of their representative immunofluorescence of kidney tissues. Of note, the abundance of Maxi-K was extremely low in both uEVs and biopsied kidney in controls but higher in GS patients, indicating that Maxi-K expression was more augmented at the high urinary flow rate.

The above-mentioned findings with an increased protein expression related to Na^+ reabsorption, K^+ secretion and regulation of acid/base balance at distal nephron from the uEVs in our GS patients with diminished NCC expression consisted with current idea that distal tubules including CD are highly plastic. Tubular plasticity for adaptation is defined as structural remodeling of renal tubules via cell proliferation (hyperplasia) and cell growth (hypertrophy) (43, 44). In NCC-deficient mice, early DCT showed a remarkable atrophy but CNT exhibited a marked epithelial hypertrophy accompanied by an increased apical abundance of ENaC (45). In SPAK KO mice featuring GS-like phenotypes, a distal nephron remodeling process of the CNT/CD developed to produce an increase in the numbers of principle cells and β-intercalated cells (46). These two mice models with deficient NCC clearly demonstrated the markedly attenuated DCT along with the distinctly hypertrophic and/or hyperplastic CNT/CD. Our uEVs results in GS patients were similar to those from NCC deficient animal studies, also supporting the notion of nephron plasticity with compensatory increase in the CNT/CD size.

Bulimic patients, also called pseudo-GS syndrome (47, 48), exhibiting similar laboratory and clinical features to GS, were also evaluated for disease controls. In contrast to GS patients, uEVs from bulimic patients showed a markedly enhanced abundance of NCC and p-NCC. The increased NCC and p-NCC abundance may be secondary response to volume depletion and K^+ deficiency *per se*. In rat model of K^+ deficiency, enhanced abundance NCC and p-NCC has been clearly shown (49),

closely linked to increased WNK body formation and activation of SPAK/OSR1 (50). Similarly, uEVs for upstream NHE3 and NKCC2 along with downstream ENaCβ and pendrin expression were also increased in response to salt-losing and metabolic alkalosis. Of interest, only the slightly increased ROMK and Maxi-K abundance from the isolated uEVs and biopsied kidney tissues may be associated with the interaction of bicarbonaturia to stimulate them as well as the enhanced NCC and chronic hypokalemia to suppress them.

Recently, uEVs has been emerged as a promising liquid biopsy biomarker in kidney disease research. Several novel biomarkers from uEVs including proteins, miRNA or non-coding RNA have been discovered in acute kidney injury (51, 52), chronic kidney disease (53, 54), diabetic nephropathy (55), focal segmental glomerulosclerosis (56), and lupus nephritis (57). In addition to GS and Bartter syndrome, uEVs is also utilized in some renal tubular disorders such as nephrogenic diabetes insipidus, and familial hyperkalemic hypertension due to *KLHL3* mutation (58). Accordingly, these evidence demonstrated the relevance of uEVs in understanding the pathophysiology of kidney diseases and the discovery of potential therapeutic targets. Our study provided a feasible way to analyze the differential expression proteins in renal tubular disorders and may be also applied to other non-tubular disorder such as cisplatin or drug induced tubulopathy.

There were some limitations of this study. First, the sample size of GS patients was still small due to the restricted loading wells of SDS/PAGE for immunoblotting. Second, other relevant transporters along the renal tubules such as TRPV5 and TRPM6 were not examined because of limited uEVs proteins isolated from ultracentrifugation. Third, the localization of these transporters in renal tubules could not be identified using uEVs. Finally, the specificity and sensitivity of the antibodies used for this study might affect expression of renal transporters between immunoblotting and immunofluorescence (for example NKCC2). Using the detergent for immunoblotting is another approach to enhance intracellular epitope recognition in uEVs (22).

In conclusion, uEVs could be used as non-invasive diagnostic tool to evaluate the renal tubular Na^+ or K^+ associated transporters expression in GS patients. High-throughput proteomic studies from uEVs in GS patients will be anticipated in the further investigation.

DATA AVAILABILITY STATEMENT

The original contributions presented in the study are included in the article/supplementary material, further inquiries can be directed to the corresponding author/s.

ETHICS STATEMENT

The studies involving human participants were reviewed and approved by Institutional Review Board of the Tri-Service General Hospital of Taiwan (TSGHIRB No.2-103-05-160 and TSGHIRB No.2-105-05-062). The patients/participants provided their written informed consent to participate in this study.

AUTHOR CONTRIBUTIONS

C-CS, M-HC, and S-HL substantially contributed to study conception and design, acquisition of data, and analysis and interpretation of data. Y-ChaL, Y-ChuL, Y-JL, and S-SY substantially contributed to acquisition of data, and analysis and interpretation of data. All the authors revised the paper and approved the final version of the article to be published.

FUNDING

This research was supported by grants from the Research Fund of the Ministry of Science and Technology (MOST) of Taiwan (MOST 104-2314-B-016-021-MY2 and MOST 106-2314-B-016-033-MY3) and the Research Fund of the Tri-Service General Hospital (TSGH-C107-007-S04, TSGH-C108-007-S04, and TSGH-C108-027).

ACKNOWLEDGMENTS

The authors acknowledge technical services provided by Instrument Center of National Defense Medical Center.

REFERENCES

1. Blanchard A, Bockenhauer D, Bolignano D, Calò LA, Cosyns E, Devuyst O, et al. Gitelman syndrome: consensus and guidance from a Kidney Disease: Improving Global Outcomes (KDIGO) Controversies Conference. *Kidney Int.* (2017) 91:24–33. doi: 10.1016/j.kint.2016.09.046
2. Simon DB, Nelson-Williams C, Bia MJ, Ellison D, Karet FE, Molina AM, et al. Gitelman's variant of Bartter's syndrome, inherited hypokalaemic alkalosis, is caused by mutations in the thiazide-sensitive Na-Cl cotransporter. *Nat Genet.* (1996) 12:24–30. doi: 10.1038/ng0196-24
3. Lo Y-F, Nozu K, Iijima K, Morishita T, Huang C-C, Yang S-S, et al. Recurrent deep intronic mutations in the SLC12A3 gene responsible for Gitelman's syndrome. *Clin J Am Soc Nephrol.* (2011) 6:630–9. doi: 10.2215/CJN.06730810
4. Vargas-Poussou R, Dahan K, Kahila D, Venisse A, Riveira-Munoz E, Debaix H, et al. Spectrum of mutations in Gitelman syndrome. *J Am Soc Nephrol.* (2011) 22:693–703. doi: 10.1681/ASN.2010090907
5. Tseng MH, Yang SS, Hsu YJ, Fang YW, Wu CJ, Tsai JD, et al. Genotype, phenotype, and follow-up in Taiwanese patients with salt-losing tubulopathy associated with SLC12A3 mutation. *J Clin Endocrinol Metab.* (2012) 97:E1478–82. doi: 10.1210/jc.2012-1707
6. Yang SS, Lo YF, Yu IS, Lin SW, Chang TH, Hsu YJ, et al. Generation and analysis of the thiazide-sensitive Na+ -Cl- cotransporter (Ncc/Slc12a3) Ser707X knockin mouse as a model of Gitelman syndrome. *Hum Mutat.* (2010) 31:1304–15. doi: 10.1002/humu.21364
7. van Balkom BW, Pisitkun T, Verhaar MC, Knepper MA. Exosomes and the kidney: prospects for diagnosis and therapy of renal diseases. *Kidney Int.* (2011) 80:1138–45. doi: 10.1038/ki.2011.292
8. Pisitkun T, Shen RF, Knepper MA. Identification and proteomic profiling of exosomes in human urine. *Proc Natl Acad Sci USA.* (2004) 101:13368–73. doi: 10.1073/pnas.0403453101
9. Gonzales P, Pisitkun T, Knepper MA. Urinary exosomes: is there a future? *Nephrol Dial Transplant.* (2008) 23:1799–801. doi: 10.1093/ndt/gfn058

10. Knepper MA, Pisitkun T. Exosomes in urine: who would have thought? *Kidney Int.* (2007) 72:1043–5. doi: 10.1038/sj.ki.5002510
11. Bonifacino JS, Traub LM. Signals for sorting of transmembrane proteins to endosomes and lysosomes. *Annu Rev Biochem.* (2003) 72:395–447. doi: 10.1146/annurev.biochem.72.121801.161800
12. Gonzales PA, Pisitkun T, Hoffert JD, Tchapyjnikov D, Star RA, Kleta R, et al. Large-scale proteomics and phosphoproteomics of urinary exosomes. *J Am Soc Nephrol.* (2009) 20:363–79. doi: 10.1681/ASN.2008040406
13. van der Lubbe N, Jansen PM, Salih M, Fenton RA, van den Meiracker AH, Danser AH, et al. The phosphorylated sodium chloride cotransporter in urinary exosomes is superior to prostasin as a marker for aldosteronism. *Hypertension.* (2012) 60:741–8. doi: 10.1161/HYPERTENSIONAHA.112.198135
14. Salih M, Fenton RA, Zietse R, Hoorn EJ. Urinary extracellular vesicles as markers to assess kidney sodium transport. *Curr Opin Nephrol Hypertens.* (2016) 25:67–72. doi: 10.1097/MNH.0000000000000192
15. Salih M, Bovée DM, van der Lubbe N, Danser AHJ, Zietse R, Feelders RA, et al. Increased urinary extracellular vesicle sodium transporters in Cushing syndrome with hypertension. *J Clin Endocrinol Metab.* (2018) 103:2583–91. doi: 10.1210/jc.2018-00065
16. Wolley MJ, Wu A, Xu S, Gordon RD, Fenton RA, Stowasser M. In primary aldosteronism, mineralocorticoids influence exosomal sodium-chloride cotransporter abundance. *J Am Soc Nephrol.* (2017) 28:56–63. doi: 10.1681/ASN.2015111221
17. Corbetta S, Raimondo F, Tedeschi S, Syrèn ML, Rebora P, Savoia A, et al. Urinary exosomes in the diagnosis of Gitelman and Bartter syndromes. *Nephrol Dial Transplant.* (2015) 30:621–30. doi: 10.1093/ndt/gfu362
18. Isobe K, Mori T, Asano T, Kawaguchi H, Nonoyama S, Kumagai N, et al. Development of enzyme-linked immunosorbent assays for urinary thiazide-sensitive Na-Cl cotransporter measurement. *Am J Physiol Renal Physiol.* (2013) 305:F1374–81. doi: 10.1152/ajprenal.00208.2013
19. Vahia VN. Diagnostic and statistical manual of mental disorders 5: a quick glance. *Indian J Psychiatry.* (2013) 55:220–3. doi: 10.4103/0019-5545.117131
20. Sokolova V, Ludwig AK, Hornung S, Rotan O, Horn PA, Epple M, et al. Characterisation of exosomes derived from human cells by nanoparticle tracking analysis and scanning electron microscopy. *Colloids Surf B Biointerfaces.* (2011) 87:146–50. doi: 10.1016/j.colsurfb.2011.05.013
21. Abdeen A, Sonoda H, Oshikawa S, Hoshino Y, Kondo H, Ikeda M. Acetazolamide enhances the release of urinary exosomal aquaporin-1. *Nephrol Dial Transplant.* (2016) 31:1623–32. doi: 10.1093/ndt/gfw033
22. Blijdorp CJ, Tutakhel OAZ, Hartjes TA, van den Bosch TPP, van Heugten MH, Rigalli JP, et al. Comparing approaches to normalize, quantify, and characterize urinary extracellular vesicles. *J Am Soc Nephrol.* (2021) 32:1210–26. doi: 10.1681/ASN.2020081142
23. Yang SS, Fang YW, Tseng MH, Chu PY, Yu IS, Wu HC, et al. Phosphorylation regulates NCC stability and transporter activity in vivo. *J Am Soc Nephrol.* (2013) 24:1587–97. doi: 10.1681/ASN.2012070742
24. Joo KW, Lee JW, Jang HR, Heo NJ, Jeon US, Oh YK, et al. Reduced urinary excretion of thiazide-sensitive Na-Cl cotransporter in Gitelman syndrome: preliminary data. *Am J Kidney Dis.* (2007) 50:765–73. doi: 10.1053/j.ajkd.2007.07.022
25. Jang HR, Lee JW, Oh YK, Na KY, Joo KW, Jeon US, et al. From bench to bedside: diagnosis of Gitelman's syndrome – defect of sodium-chloride cotransporter in renal tissue. *Kidney Int.* (2006) 70:813–7. doi: 10.1038/sj.ki.5001694
26. Syrén ML, Tedeschi S, Cesareo L, Bellantuono R, Colussi G, Procaccio M, et al. Identification of fifteen novel mutations in the SLC12A3 gene encoding the Na-Cl Co-transporter in Italian patients with Gitelman syndrome. *Hum Mutat.* (2002) 20:78. doi: 10.1002/humu.9045
27. De Jong JC, Van Der Vliet WA, Van Den Heuvel LP, Willems PH, Knoers NV, Bindels RJ. Functional expression of mutations in the human NaCl cotransporter: evidence for impaired routing mechanisms in Gitelman's syndrome. *J Am Soc Nephrol.* (2002) 13:1442–8. doi: 10.1097/01.ASN.0000017904.77985.03
28. Knepper MA, Brooks HL. Regulation of the sodium transporters NHE3, NKCC2 and NCC in the kidney. *Curr Opin Nephrol Hypertens.* (2001) 10:655–9. doi: 10.1097/00041552-200109000-00017
29. Bobulescu IA, Moe OW. Na^+/H^+ exchangers in renal regulation of acid-base balance. *Semin Nephrol.* (2006) 26:334–44. doi: 10.1016/j.semnephrol.2006.07.001
30. Fenton RA, Poulsen SB, de la Mora Chavez S, Soleimani M, Dominguez Rieg JA, Rieg T. Renal tubular NHE3 is required in the maintenance of water and sodium chloride homeostasis. *Kidney Int.* (2017) 92:397–414. doi: 10.1016/j.kint.2017.02.001
31. Elkjaer ML, Kwon TH, Wang W, Nielsen J, Knepper MA, Frøkiaer J, et al. Altered expression of renal NHE3, TSC, BSC-1, and ENaC subunits in potassium-depleted rats. *Am J Physiol Renal Physiol.* (2002) 283:F1376–88. doi: 10.1152/ajprenal.00186.2002
32. Khuri RN, Strieder WN, Giebisch G. Effects of flow rate and potassium intake on distal tubular potassium transfer. *Am J Physiol.* (1975) 228:1249–61. doi: 10.1152/ajplegacy.1975.228.4.1249
33. Malnic G, Berliner RW, Giebisch G. Flow dependence of K^+ secretion in cortical distal tubules of the rat. *Am J Physiol.* (1989) 256 (5 Pt 2):F932–41. doi: 10.1152/ajprenal.1989.256.5.F932
34. Wall SM, Verlander JW, Romero CA. The renal physiology of pendrin-positive intercalated cells. *Physiol Rev.* (2020) 100:1119–47. doi: 10.1152/physrev.00011.2019
35. Soleimani M, Barone S, Xu J, Shull GE, Siddiqui F, Zahedi K, et al. Double knockout of pendrin and Na-Cl cotransporter (NCC) causes severe salt wasting, volume depletion, and renal failure. *Proc Natl Acad Sci USA.* (2012) 109:13368–73. doi: 10.1073/pnas.1202671109
36. Subramanya AR, Ellison DH. Distal convoluted tubule. *Clin J Am Soc Nephrol.* (2014) 9:2147–63. doi: 10.2215/CJN.05920613
37. Hebert SC. An ATP-regulated, inwardly rectifying potassium channel from rat kidney (ROMK). *Kidney Int.* (1995) 48:1010–6. doi: 10.1038/ki.1995.383
38. Lee WS, Hebert SC. ROMK inwardly rectifying ATP-sensitive K+ channel. I. Expression in rat distal nephron segments. *Am J Physiol.* (1995) 268 (6 Pt 2):F1124–31. doi: 10.1152/ajprenal.1995.268.6.F1124
39. Giebisch G. Renal potassium transport: mechanisms and regulation. *Am J Physiol.* (1998) 274:F817–33. doi: 10.1152/ajprenal.1998.274.5.F817
40. Welling PA, Ho K. A comprehensive guide to the ROMK potassium channel: form and function in health and disease. *Am J Physiol Renal Physiol.* (2009) 297:F849–63. doi: 10.1152/ajprenal.00181.2009
41. Pluznick JL, Sansom SC. BK channels in the kidney: role in K(+) secretion and localization of molecular components. *Am J Physiol Renal Physiol.* (2006) 291:F517–29. doi: 10.1152/ajprenal.00118.2006
42. Rodan AR, Huang CL. Distal potassium handling based on flow modulation of maxi-K channel activity. *Curr Opin Nephrol Hypertens.* (2009) 18:350–5. doi: 10.1097/MNH.0b013e32832c75d8
43. Kaissling B, Bachmann S, Kriz W. Structural adaptation of the distal convoluted tubule to prolonged furosemide treatment. *Am J Physiol.* (1985) 248 (3 Pt 2):F374–81. doi: 10.1152/ajprenal.1985.248.3.F374
44. Kaissling B, Stanton BA. Adaptation of distal tubule and collecting duct to increased sodium delivery. I. Ultrastructure. *Am J Physiol.* (1988) 255 (6 Pt 2):F1256–68. doi: 10.1152/ajprenal.1988.255.6.F1256
45. Loffing J, Vallon V, Loffing-Cueni D, Aregger F, Richter K, Pietri L, et al. Altered renal distal tubule structure and renal Na^+ and Ca^{2+} handling in a mouse model for Gitelman's syndrome. *J Am Soc Nephrol.* (2004) 15:2276–88. doi: 10.1097/01.ASN.0000138234.18569.63
46. Grimm PR, Lazo-Fernandez Y, Delpire E, Wall SM, Dorsey SG, Weinman EJ, et al. Integrated compensatory network is activated in the absence of NCC phosphorylation. *J Clin Invest.* (2015) 125:2136–50. doi: 10.1172/JCI78558
47. Seyberth HW, Schlingmann KP. Bartter- and Gitelman-like syndromes: salt-losing tubulopathies with loop or DCT defects. *Pediatr Nephrol.* (2011) 26:1789–802. doi: 10.1007/s00467-011-1871-4
48. Matsunoshita N, Nozu K, Shono A, Nozu Y, Fu XJ, Morisada N, et al. Differential diagnosis of Bartter syndrome, Gitelman syndrome, and pseudo-Bartter/Gitelman syndrome based on clinical characteristics. *Genet Med.* (2016) 18:180–8. doi: 10.1038/gim.2015.56
49. Frindt G, Palmer LG. Effects of dietary K^+ on cell-surface expression of renal ion channels and transporters. *Am J Physiol Renal Physiol.* (2010) 299:F890–7. doi: 10.1152/ajprenal.00323.2010
50. Wade JB, Liu J, Coleman R, Grimm PR, Delpire E, Welling PA. SPAK-mediated NCC regulation in response to low-K+ diet. *Am J Physiol Renal Physiol.* (2015) 308:F923–31. doi: 10.1152/ajprenal.00388.2014

51. Sonoda H, Lee BR, Park K-H, Nihalani D, Yoon J-H, Ikeda M, et al. miRNA profiling of urinary exosomes to assess the progression of acute kidney injury. *Scientific Reports.* (2019) 9:4692. doi: 10.1038/s41598-019-40747-8
52. Awdishu L, Tsunoda S, Pearlman M, Kokoy-Mondragon C, Ghassemian M, Naviaux RK, et al. Identification of maltase glucoamylase as a biomarker of acute kidney injury in patients with cirrhosis. *Crit Care Res Pract.* (2019) 2019:5912804. doi: 10.1155/2019/5912804
53. Khurana R, Ranches G, Schafferer S, Lukasser M, Rudnicki M, Mayer G, et al. Identification of urinary exosomal noncoding RNAs as novel biomarkers in chronic kidney disease. *Rna.* (2017) 23:142–52. doi: 10.1261/rna.058834.116
54. Wang B, Zhang A, Wang H, Klein JD, Tan L, Wang ZM, et al. miR-26a limits muscle wasting and cardiac fibrosis through exosome-mediated microRNA transfer in chronic kidney disease. *Theranostics.* (2019) 9:1864–77. doi: 10.7150/thno.29579
55. Zang J, Maxwell AP, Simpson DA, McKay GJ. Differential expression of urinary exosomal microRNAs miR-21-5p and miR-30b-5p in individuals with diabetic kidney disease. *Sci Rep.* (2019) 9:10900. doi: 10.1038/s41598-019-47504-x
56. Gebeshuber CA, Kornauth C, Dong L, Sierig R, Seibler J, Reiss M, et al. Focal segmental glomerulosclerosis is induced by microRNA-193a and its downregulation of WT1. *Nat Med.* (2013) 19:481–7. doi: 10.1038/nm.3142
57. Garcia-Vives E, Solé C, Moliné T, Vidal M, Agraz I, Ordi-Ros J, et al. The urinary exosomal miRNA expression profile is predictive of clinical response in lupus nephritis. *Int J Mol Sci.* (2020) 21:1372. doi: 10.3390/ijms21041372
58. Salih M, Fenton RA, Knipscheer J, Janssen JW, Vredenbregt-van den Berg MS, Jenster G, et al. An immunoassay for urinary extracellular vesicles. *Am J Physiol Renal Physiol.* (2016) 310:F796–801. doi: 10.1152/ajprenal.00463.2015

Conflict of Interest: The authors declare that the research was conducted in the absence of any commercial or financial relationships that could be construed as a potential conflict of interest.